Tissue-remodelling M2 Macrophages Recruits Matrix Metalloproteinase-9 for Cryotherapy-induced Fibrotic Resolution during Keloid Treatment

Young In LEE[1,2], Soo Min KIM[1], Jihee KIM[1,2], Jemin KIM[1], Seung Yong SONG[2,3], Won Jai LEE[2,3] and Ju Hee LEE[1,2]*
Department of [1]Dermatology and [3]Plastic and Reconstructive Surgery, Severance Hospital, Cutaneous Biology Research Institute, and [2]Scar Laser and Plastic Surgery Center, Yonsei Cancer Hospital, Yonsei University College of Medicine, Seoul, Korea

Cryotherapy is used to treat keloid scars; however, the molecular and pathological mechanisms are not clearly understood. This study retrospectively evaluated the efficacy of combined treatment with cryotherapy and intralesional triamcinolone injection (Cryo+TA) or intralesional TA monotherapy (TA) in 40 Asian patients with keloid scars. Scar improvement was assessed using the Vancouver Scar Scale and Global Improvement Scale. Clinical improvement in scars, especially reduced vascularity and redness, was significantly greater in the Cryo+TA group than in the TA group. Cryotherapy-treated and untreated keloid tissue was collected from six patients for analysis. Histologically, collagen bundles from cryotherapy-treated keloid tissue were more fibrillar and abnormal thickness was reduced. Immunohistochemical staining showed a reduced number of dermal vessels after cryotherapy. Moreover, CD163$^+$ M2 macrophages and matrix metalloproteinase-9 (MMP-9) were significantly increased in cryotherapy-treated tissue. Double immunofluorescence staining revealed co-expression of CD163 and MMP-9. These data indicate that cryotherapy recruits tissue-remodelling M2 macrophages with accompanying MMP-9, suggesting that cryotherapy-recruited M2 macrophages function in fibrotic resolution during keloid treatment.

Key words: keloid scar; cryotherapy; M2 macrophage; MMP-9.

Accepted Oct 15, 2020; Epub ahead of print Oct 19, 2020

Acta Derm Venereol 2020; 100: adv00306.

Corr: Ju Hee Lee, Department of Dermatology and Cutaneous Biology Research Institute, Yonsei University College of Medicine, 50-1 Yonsei-ro, Seodaemun-gu, Seoul, Korea. E-mail: JUHEE@yuhs.ac

SIGNIFICANCE

Superficial cryotherapy is one of the most commonly used treatment modalities for keloid scars; however, its molecular mechanism is still not completely understood. This study retrospectively evaluated the efficacy of combined treatment with cryotherapy and intralesional steroid injection or intralesional steroid injection in 40 patients. Clinical scar improvement, especially improvement in redness of scars, was significantly greater when cryotherapy was combined. Histologically, abnormal collagen bundles and dermal vessels from cryotherapy-treated keloid tissue were significantly reduced. Moreover, CD163$^+$ M2 macrophages and matrix metalloproteinase-9 were significantly increased. These data indicate that cryotherapy-recruited macropahges supply matrix metalloproteinase-9, which function in fibrotic resolution in during keloid treatment.

Superficial cryotherapy is commonly used for the treatment of keloid scars, either as a monotherapy or in combination with other treatment modalities, such as intralesional triamcinolone (TA). In spite of its documented efficacy, the mechanism by which cryotherapy reduces keloid formation remains unclear. Based on previous findings, it is widely recognized that hypertrophic or keloid scars occur on burned skin, but not on frostbitten areas (1). It is hypothesized that although burning and frostbite can both lead to tissue necrosis, they induce the secretion of distinct types of proinflammatory mediators, thereby promoting different responses by tissue fibroblasts (2).

Numerous previous randomized, controlled studies have evaluated the efficacy of various keloid treatment modalities (3–6). These have revealed that keloids respond significantly better to the combined treatment of Cryo+TA, than to either TA or cryotherapy alone (7, 8). The combination of Cryo+TA promotes faster keloid tissue destruction by inducing direct cell injury and vascular damage (9). In addition, immediate tissue oedema caused by cryotherapy results in the even distribution of the steroid, thereby augmenting the effect of intralesional TA (3). Despite these intriguing observations, the molecular basis underlying the efficacy of cryotherapy is still not completely understood.

Recent studies in other organ systems, including those focused on liver fibrosis and cardiac wound healing after myocardial infarction, have shown that matrix metalloproteinase-9 (MMP-9) contributes to the resolution of fibrosis (10, 11). Specifically, these studies emphasized the role of macrophages in providing MMP-9 to the fibrotic lesion, which in turn, helps to drive the process of fibrillolysis. Macrophages are innate immune cells that display functional plasticity in the changing environment of scar development and are therefore recognized as essential mediators of wound healing (12). In particular, many studies suggest that alternatively activated (M2) macrophages secrete anti-inflammatory signals, which function to regulate tissue remodelling in a healing wound (13, 14). In contrast, the classically activated (M1)

doi: 10.2340/00015555-3665
Acta Derm Venereol 2020; 100: adv00306

macrophages display a proinflammatory phenotype and are not involved in this process.

The role of macrophages and MMP-9 in the formation and resolution of keloid scars is controversial. A study postulated a pro-fibrotic role of M2 macrophages and MMP-9 during the formation of keloid scars (15). However, contradictory results have also been published, especially during the process of keloid scar treatment. For instance, Azzam et al. (16) reported that fractional ablative laser treatment in keloid scars induced a rise in the level of MMP-9, which contributed to degradation and remodelling of collagen bundles. The current retrospective observational study on Asian keloid patients aimed to compare clinical outcomes in those treated with Cryo+TA vs patients treated with TA monotherapy. Moreover, this study aimed to evaluate the tissue histopathological events that result from cryotherapy treatment, in order to obtain molecular evidence supporting role of M2 macrophages and MMP-9 in cryotherapy-induced tissue remodelling and fibrotic resolution.

MATERIALS AND METHODS

Clinical retrospective cohort study

Study design. This study retrospectively evaluated 40 Asian patients with keloid who underwent scar treatment by experienced board-certified dermatologists in a single tertiary institution in Korea (Severance Hospital of Yonsei University Health System, Seoul). Electronic patient medical records were reviewed after approval by the Yonsei University College of Medicine Institutional Review Board (IRB number 4-2017-0470). All included patients were initially advised to undergo Cryo+TA, based on the height of the scar greater than 2 mm, presence of symptoms, such as itching/pain, and persistent spreading in size. The retrospective study was designed with 2 groups of patients who chose to receive either TA or Cryo+TA after consultation about the treatment costs, prognosis and possible side-effects. Exclusion criteria included a history of isotretinoin and immunosuppressant use, pregnancy, and those who underwent concomitant skin resurfacing procedures or laser treatments.

For administration of combination therapy, all physicians used a specialized tool called the CryoPen (L&C BIO, Gyeonggi-do, Korea), a spray-type device that, due to a freezing point of −79°C, facilitates more selective treatment than the traditional cryogun method, with fewer adverse effects on adjacent normal tissues. Three 10-s freeze-thaw cycles were performed directly over the lesions, while freezing was continued until the entire surface of the lesion became evenly white. For thicker areas of the scar greater than 5 mm in height, the CryoPen was sprayed with intermittent direct contact with the lesion. Immediately after cryotherapy, an injection of 10-mg/ml TA was administered evenly throughout the lesion. The treatment regimen was repeated on a monthly basis, until the keloid scars showed cessation of growth in size, complete flattening, and absence of symptoms.

Clinical assessments. Digital photographs were obtained prior to each treatment session using identical camera settings and lighting conditions. Scars had been routinely evaluated at the clinic using the Vancouver Scar Scale (VSS) to record changes in pigmentation, pliability, height, and vascularity (scores are listed in Table SI[1]). The VSS along the treatment periods were retrospectively reviewed from the subjects' medical records on every visit. Meanwhile, 2 independent board-certified dermatologists were provided with clinical photographs from the initial and final visits of each patient. They were then asked to assign scores on scar improvement for the patients using 5-point Global Improvement Scale (GIS): 5 = very much improved, 4 = much improved, 3 = improved, 2 = no change, and 1 = worse.

Histological analysis of the effect of cryotherapy on keloid scar treatment

Tissue preparation. Keloid tissues ($n = 6$) were obtained from patients who had been previously scheduled for surgical excision at the Department of Plastic and Reconstructive Surgery, Yonsei University College of Medicine (their keloid characteristics are described in Table SII[1]). Tissues were obtained according to a protocol approved by the Yonsei Institutional Review Board (4-2017-0259), and all patients provided written informed consent. Each keloid lesion was divided into a cryotherapy-treated area and an untreated control area. Superficial cryotherapy was then performed on the cryotherapy-treated area 2 weeks prior to the surgery, according to the protocol described above. Both cryotherapy-treated and untreated keloid tissues were collected, and immunohistochemistry and western blot analysis were performed.

Histological analysis. Paraffin blocks containing surgically excised keloid tissues were cut into 4-μm thick sections, and these were deparaffinized and dehydrated using a xylene and ethanol series. Samples were stained with haematoxylin and eosin (H&E) and the Masson's Trichrome (MT) Stain Kit (ab150686, Abcam, Cambridge, MA, USA), according to the manufacturer's instructions.

Immunohistochemistry. Consecutively sectioned tissue samples from paraffin blocks were deparaffinized by xylene. Sections were soaking in descending alcohol. The tissue sections were boiled in citrate buffer (pH 6; Sigma-Aldrich, St Louis, MO, USA) for antigen retrieval. Samples were then incubated with 3% H_2O_2 on ice for 10 min, followed by a blocking step with 5% skim milk in Tris-buffered saline with tween 20 (TBS-T). Primary antibodies, including anti-MMP-9 (1:100, ab38898; Abcam), anti-CD68 (1:500, ab213363; Abcam), anti-CD163 (1:500, ab156769; Abcam), anti-iNOS (1:20, ab3523; Abcam), and anti-TIMP1 (1:1000, ab211926; Abcam) were applied to the samples, and these were incubated at 4°C overnight. CD68 is used as a marker for cells of the monocyte lineage including tissue macrophages; CD163 and iNOS were used as specific monocyte/macrophage marker for M2 and M1 macrophages, respectively. Primary antibodies were detected using the ChemMate EnVision Detection Kit (K5007; DAKO, Carpinteria, CA, USA). The slides were incubated and developed with the secondary antibody for 30 min and 3,3-diaminobenzidine for 5 min, followed by counterstaining using Gill's haematoxylin. Double immunofluorescence staining with CD163 and MMP-9 was used to determine cell localization of MMP-9. The primary antibodies used were as follows: rabbit anti-MMP9 (1:1,000) and mouse anti-CD163 (1:100). After 24 h of co-incubation, sections were washed with PBS and incubated with secondary antibodies for 1 h. Then sections sealed with 50% glycerol were observed and photographed under fluorescence microscopy. Image analysis for the semi-quantitative measurements of immunohistochemistry-stained keloid sections was performed using Image J software (National Institutes of Health, Bethesda, MD, USA). All analyses were performed on images (original magnification, 100×) generated from 5 tissue sections of each study group, and the mean data was used for statistical analysis.

Western blot analysis. Tissue samples were homogenized using a mechanical TissueLyser II (QIAGEN, Hilden, Germany) with stainless steel beads at 30 Hz for 3 min. Cells were lysed with

[1]https://doi.org/10.2340/00015555-3665

RIPA buffer, and protein concentrations were determined using the BCA Protein Assay Kit (Sigma-Aldrich). Total protein (30 µg) was separated by 8% or 10% SDS-PAGE and then transferred to nitrocellulose blotting membranes (GE Healthcare, Dornstadt, Germany). Membranes were blocked in 5% skim milk and treated with the following primary antibodies for 17 h at 4°C: anti-β-actin (1:1000, SC-47778, Santa Cruz Biotechnology, Dallas, TX, USA), anti-CD68 (1:1000, ab213363; Abcam), anti-MMP-2 (1:1,000, #4022s; Cell Signaling Technology, Beverly, MA, USA), anti-MMP-9 (1:1,000, #3852s; Cell Signaling Technology), and anti-CD163 (1:1,000, ab156769; Abcam). Membranes were washed 3 times with TBS-T and treated with the secondary antibodies, anti-mouse IgG (1:2,000, SC-2005; Santa Cruz Biotechnology) and anti-rabbit IgG (1:2,000, #7074S; Cell signaling Technology), for 2 h at room temperature. These were then washed 3 times with TBS-T and treated with a chemiluminescence (ECL) detection reagent (Ab Frontier, Seoul, Korea). The resulting bands were visualized and quantified using the LAS-4000 mini luminescence image analyser (Fujifilm Life Sciences, Tokyo, Japan).

Statistical analysis

Data are shown as mean ± standard error of the mean (SEM) and were analysed for the retrospective cohort study using Student's *t*-tests. Statistical differences for the histological study were determined using a non-parametric Mann–Whitney *U* test. $p < 0.001$ (***), $p < 0.01$ (**), and $p < 0.05$ (*) were considered statistically significant. SPSS v. 23.0 (SPSS Inc., Chicago, IL, USA) was used for all statistical analyses.

RESULTS

Patient information and demographic characteristics

This study retrospectively identified patients with keloid scars who visited our dermatology clinic between January 2017 and January 2019 (**Table I**). The study included 40 Asian patients (17 males, 23 females), all of whom had initially been recommended for combination treatment with Cryo+TA, based on the scar's thickest height > 2 mm, presence of symptoms, and persistence in the spread of size. Twenty study patients subsequently chose to receive TA monotherapy. The mean number of clinic visits for all patients was 14.8 sessions (range 7–25 sessions) in monthly intervals. Comparison of the 2 treatment groups revealed that the mean number of visits was 12.7 ± 0.9 for Cryo+TA and 16.3 ± 1.1 for TA ($p = 0.023$). Only 3 patients from the Cryo+TA group and 4 from the TA group revisited the clinic for the one-year follow-up after the last treatment. Their medical records showed stable disease status without recurrence of active scar proliferation. The mean treatment period was 13.1 ± 0.9 months for Cryo+TA and 16.7 ± 1.0 months for TA ($p = 0.017$). Thus, both the number of visits and the duration of treatment were significantly greater for the TA group. No missing values were observed in this retrospective cohort study. No significant differences were found in age, sex, or

Table I. Retrospective study patient demographics

	TA monotherapy	Cryo+TA	*p*-value
Age, years, mean ± SEM	44.1 ± 3.7	43.8 ± 4.6	0.960
Sex, *n*			0.115
Male	11	6	
Female	9	14	
Location of scar, *n*			0.531
Stretch-prone[a]	7	11	
Stretch-free[b]	13	9	
Number of treatments (sessions), mean ± SD	13.6 ± 1.0	9.1 ± 0.8	**0.001**
Duration of treatments (months), mean ± SD	16.7 ± 1.0	13.0 ± 0.8	**0.009**

[a]Stretch-prone areas included in the study: chest, shoulder, forearm, lower extremities. [b]Stretch-free areas included in the study: earlobe, head and neck, abdomen, buttock.
SEM: standard error of mean; TA: triamcinolone injection Cryo: cryotherapy. **[AQ7]**

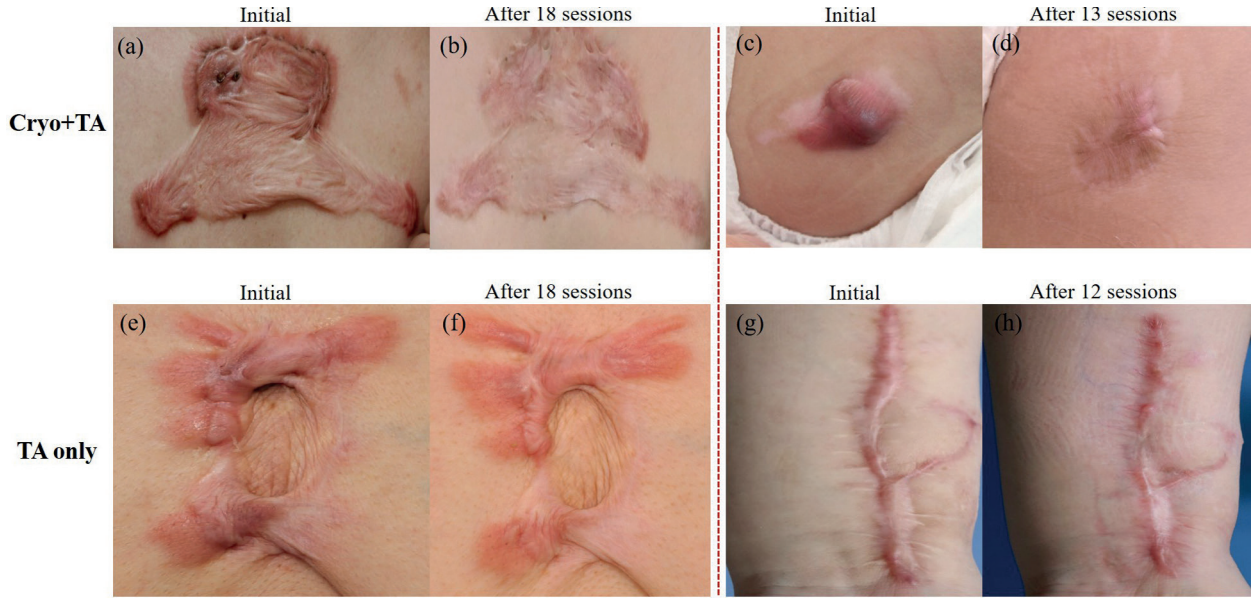

Fig. 1. Photographic comparison of clinical outcomes in keloid patients administered combined treatment with cryotherapy and triamcinolone (Cryo+TA) or triamcinolone (TA) monotherapy. (a, c) Initial and (b, d) post-treatment photographs of patients in the Cryo+TA group. (e, g) Initial and (f, h) post-treatment photographs of patients in the TA group.

Table II. Clinical improvement assessment of Vancouver Scar Scale (VSS) and Global Improvement Scale (GIS) between triamcinolone injection (TA) and cryotherapy and triamcinolone (Cryo+TA)

	TA Mean ± SEM	Cryo+TA Mean ± SEM	*p*-value
Improvement in VSS ($VSS_{initial}$-VSS_{post})			
Total VSS	2.95 ± 0.36	4.65 ± 0.41	**0.003**
Vascularity	0.05 ± 0.15	1.95 ± 0.15	**<0.001**
Pliability	2.00 ± 0.20	1.55 ± 0.18	0.111
Height	0.90 ± 0.16	1.15 ± 0.16	0.287
GIS	3.35 ± 0.15	4.05 ± 0.17	**0.004**

SEM: standard error of mean. *p*-values in bold indicates $p < 0.05$.

anatomical site (stretch-prone, stretch-free) distributions between the study groups.

Clinical improvement assessments

Clinical improvement was assessed in all subjects using the VSS (see Table SIII[1]). The result showed that the mean change in total VSS after treatment for the Cryo+TA group was 4.65 ± 0.41, whereas the mean change in total VSS for the TA group was 2.95 ± 0.36 ($p = 0.003$, **Fig. 1, Table II**). These data indicate a significantly greater improvement in total VSS for the Cryo+TA group relative to the TA group. Scores from individual VSS subcategories (pigmentation, vascularity, pliability, and height) were then analysed and it was found that the mean change in vascularity score after treatment was significantly greater for Cryo+TA (1.95 ± 0.15) than for TA (0.05 ± 0.15; $p < 0.001$). In contrast, no significant differences in the observed improvements in pliability, height, and pigmentation between the Cryo+TA and the TA groups were detected (Table II). Scars from each treatment group were also evaluated using the GIS. The mean GIS score was 4.05 ± 0.17 for Cryo+TA, and 3.35 ± 0.15 for TA, indicating a significantly greater improvement for Cryo+TA ($p = 0.004$).

Histopathological analysis of collagen in keloid scars treated with cryotherapy

The histological features of cryotherapy-treated keloid tissues and untreated controls were then using immunohistochemistry (IHC) and western blot analysis in 6 surgically-excised keloid scars. Notably, H&E staining revealed excessive and abnormally thick bundles of collagen fibres in the upper to mid-dermis of untreated lesions (**Fig. 2**a, b). These thick bundles were rarely detected in cryotherapy-treated tissues; they appeared more fibrillar, and the thickness of the abnormal collagen bundles was largely reduced relative to the untreated lesion (Fig. 2d, e). Masson's trichrome staining of the cryotherapy-treated tissue showed replacement of the dense and thick collagen bundles by fine and shallow collagen. This apparent reduction in collagen expression in response to cryotherapy treatment was also confirmed by the semi-quantitative measurement ($p < 0.0001$, **Fig.**

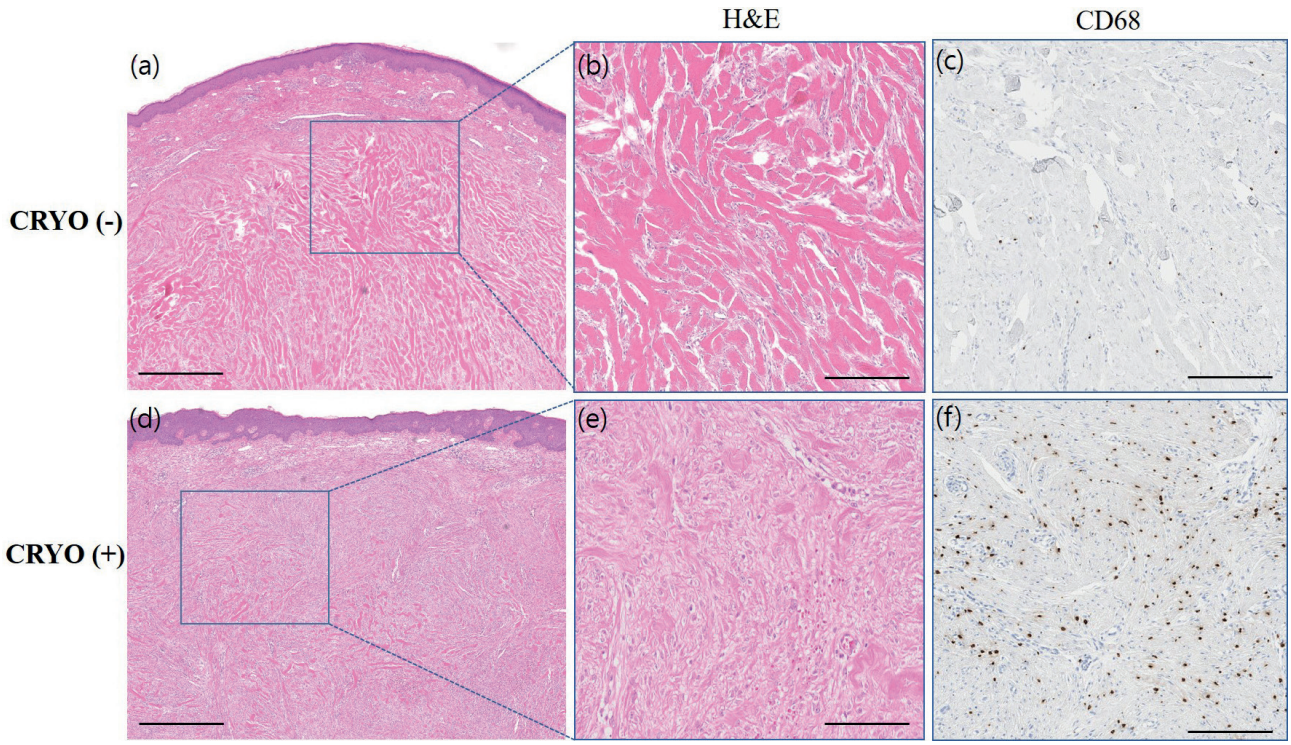

Fig. 2. Histologic analysis of keloids treated with cryotherapy. Hematoxylin and eosin (H&E) staining of (a, b) untreated keloid shows thick bundles of collagen fibers (scale bar =1 mm in lower magnification and 200 μm in higher magnification). Cryotherapy-treated keloid (d, e) reveals replacement of abnormal collagen by fine collagen, as well as the infiltration of large round cells with elongated nuclei. Immunohistochemical staining (c, f) reveals that these infiltrated cells are $CD68^+$ macrophages. Original maginification x25 and x100.

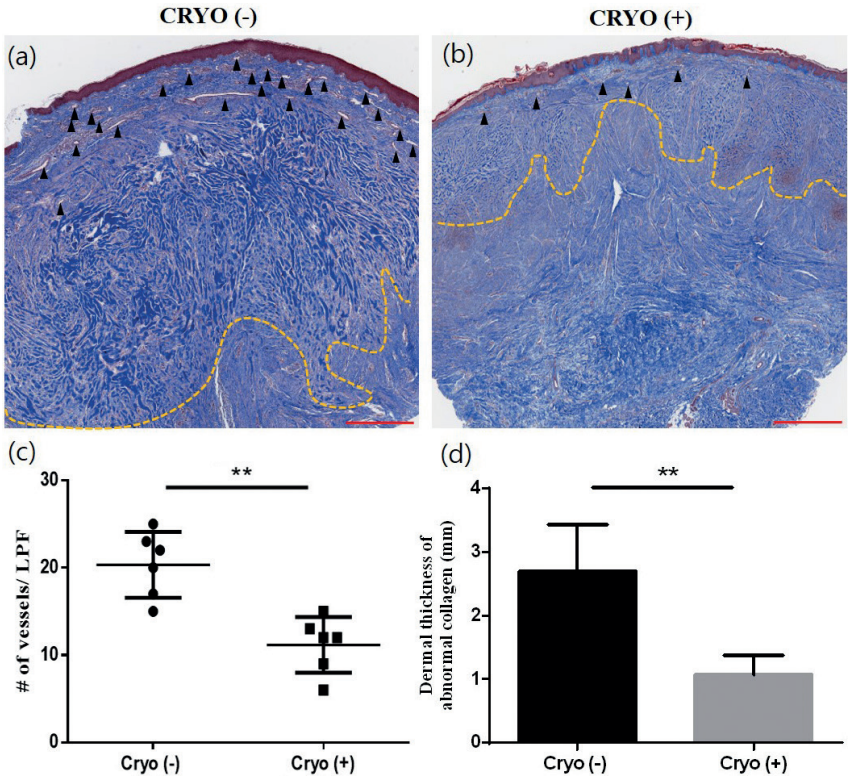

Fig. 3. Masson's trichrome staining shows decreased number of dermal vessels and thickened collagen bundle after cryotherapy. Masson's trichrome staining of (a) cryotherapy-untreated tissue and (b) cryotherapy-treated tissue (scale bar indicates 1 mm, orginical magnification x25). (c) Comparison on the number of dermal blood vessels and (d) the dermal thickness of abnormal collagen bundles on cryo (-) and cryo (+) keloid tissues (arrow heads point blood vessels; dotted lines indicate dermal thickness showing abnormal collagen; $^{**}p < 0.01$).

3a, b). Moreover, the reductions in the number of blood vessels and the dermal thickness of abnormal collagen (determined as the distance between the uppermost and the deepest portion of densely stained collagen) were measured between cryotherapy-untreated and cryotherapy-treated tissues ($p < 0.01$, Fig. 3c, d). These results correlate with the clinical improvement in the redness and height of keloid scars after Cryo+TA.

Immunohistochemistry and western blot analysis revealed an increased number of M2 macrophages and elevated MMP-9 levels in cryotherapy-treated tissue

Interestingly, H&E staining not only showed decreased collagen thickness in cryotherapy-treated tissue, but also revealed the infiltration of large round cells resembling macrophages with lightly stained elongated nuclei in-between the fine collagen bundles. To identify these cells, IHC staining with anti-CD68 antibodies was performed, which confirmed that cryotherapy-treated regions of keloid scars are populated by infiltrating macrophages (Fig. 2c, f). These cells were also positively stained with anti-CD163 antibodies, indicating that they belonged to the M2-like macrophage subtype (**Fig. 4**a–d). The additional IHC staining with anti-iNOS antibodies (markers for M1 macrophages) and anti-TIMP -1 antibodies showed no significant difference between control and cryotherapy-treated tissues (data not shown).

Immunostaining with antibodies to MMP-9 was performed and higher expression of positive brown staining was detected in the dermis of cryotherapy-treated tissue compared with control (Fig. 4e–h). To further confirm these observations, semi-quantitative analysis was conducted, which showed that the levels of both CD163 (*green*) and MMP (*red*) are significantly increased in cryotherapy-treated tissue relative to control tissue ($p < 0.0001$). Double immunofluorescence staining revealed co-expression of CD163 and MMP-9, suggesting a fibrinolytic role of M2 macrophages by the production of MMP-9 (Fig. 4 k, 1). Total protein extracts from excised keloid tissue were also analysed by western blot and a consistent pattern was observed, with increased expression of CD68, CD163 and MMP-9 in cryotherapy-treated vs control tissue (**Fig. 5**).

DISCUSSION

Cryotherapy, combined with intralesional TA, is one of the traditional first-line treatments for treating keloid scars. Intralesional TA injection diminishes excessive collagen synthesis and inhibits the rapid growth of keloid fibroblasts (17). Moreover, corticosteroid also controls the exaggerated local inflammatory processes in wound healing, thereby preventing keloid formation (18). Cryotherapy prior to TA injection not only induces early flattening of the lesion via microvascular damage, which results from the thawing phase and consequent vessel thrombosis, but also causes slight tissue oedema, which allows even distribution of the injected steroid (3). In addition, direct cellular injury due to the formation

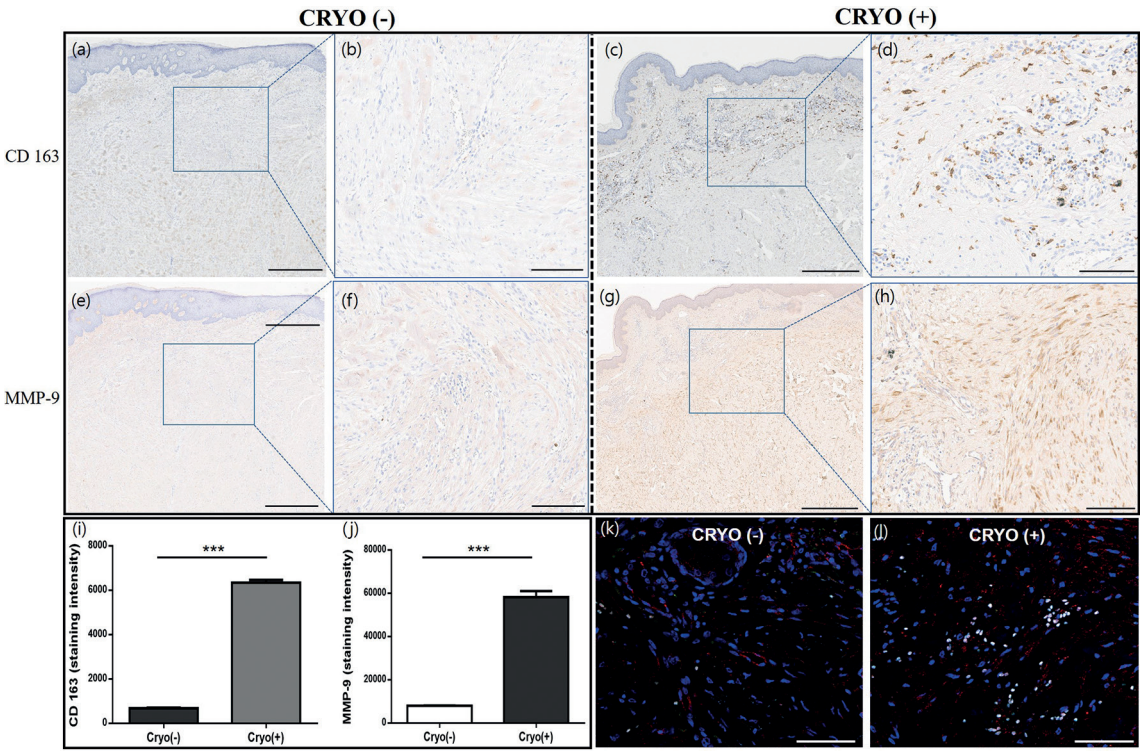

Fig. 4. Immunohistochemical staining reveals the infiltration of M2 macrophages and recruitment of MMP-9 after cryotherapy. CD163$^+$ macrophages in (a, b) cryotherapy-untreated tissue shows few positive cells, as compared to (c, d) cryotherapy-treated keloid lesion (CD163 staining, orginical magnifications x25 and x100). MMP-9 immunoreactivity in (e, f) cryotherapy-untreated and (g, h) cryotherapy-treated tissue reveals increase in MMP-9 after cryotherapy (MMP-9 staining, scale bar indicates 1 mm in lower magnification and 200 μm in higher magnification, orginical magnifications x25 and x100). (i) Percentage of positive area of CD163 and (j) MMP-9 (**$p < 0.01$). Double immunofluorescence staining shows co-expression of CD 163 (green) and MMP-9 (red) in (k) cryotherapy-untreated and (l) cryotherapy-treated tissues (scale bar indicates 50 μm, original magnification x50).

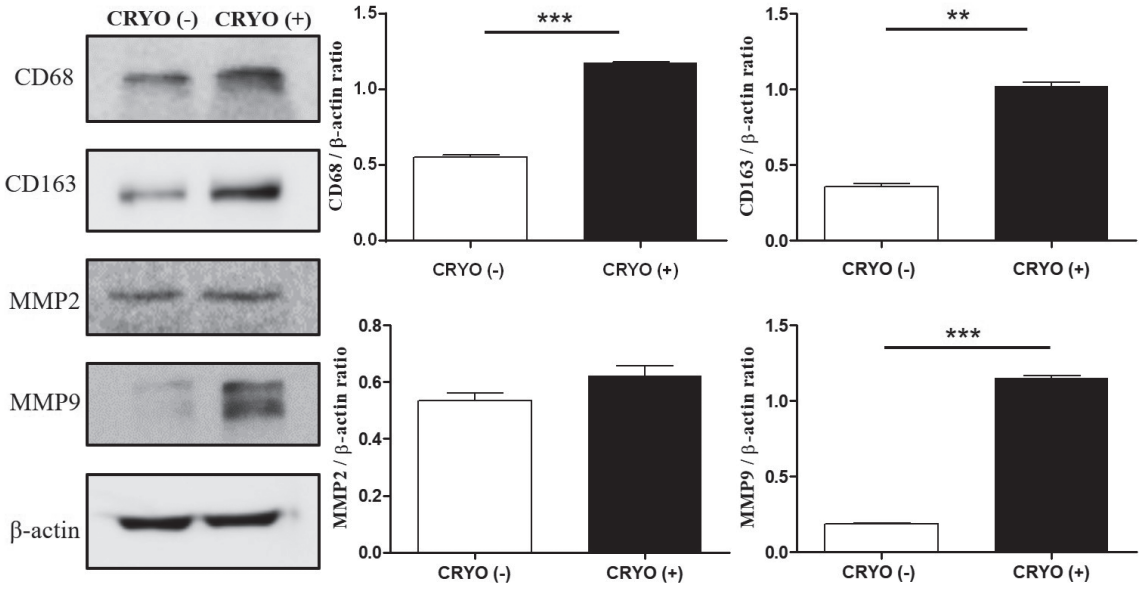

Fig. 5. Quantitative western blot analysis confirms increased expression of CD68, CD163, and matrix metalloproteinase-9 (MMP-9) in cryotherapy-treated keloid tissue relative to untreated control tissue.

of ice crystals, which remove water from the cell, also promotes subsequent tissue destruction.

This retrospective study compared the efficacy of monthly Cryo+TA vs TA for the treatment of keloid scars in 40 Asian patients. Conventionally, TA injection is given every 2–6 weeks; in the current study the TA group received monthly TA monotherapy, as the patients showed keloids with active inflammatory borders, while displaying symptoms such as itching and pain. Clinically, significantly greater improvements in total VSS and GIS scores were detected for the Cryo+TA group compared with the TA group. In particular, reduction in erythema was significantly greater in the Cryo+TA group, possibly due to efficient microvascular injury from adjuvant cryotherapy. The subsequent histopathological analysis also revealed a decreased number of blood vessels and decreased dermal thickness of abnormal collagen, thereby supporting the clinical results. Because of the possible limitations of a retrospective cohort study design, future confirmation of this finding by means of a prospective, randomized study is advisable.

A previous controlled study on the effect of cryotherapy reported that spray-type cryotherapy was clinically ineffective as a monotherapy (19). Here, we speculate that these conflicting results are probably due not only to the use of cryotherapy in combination with intralesional TA in our study, but also possibly to the differences in how we used the CryoPen. Specifically, we performed 3 well-retained freeze-thaw cycles with the CryoPen. Freezing was conducted for 10 s above the lesion, until the entire surface of the lesion became evenly white. On thicker areas of the scars, the CryoPen was also sprayed with intermittent direct contact to the lesion. This method creates an instant negative pressure formed between the tip of CryoPen and the scar, causing the scar tissue to be pulled up so that the lesion is slightly detached from the bottom tissue, therefore loosening the fibrotic spaces. Moreover, the thawing phase was strictly maintained for multiple seconds until the lesion colour returned to normal, which could allow adequate microvascular injury, leading to hypoxia and consequent tissue reduction.

Although the physical mechanisms by which cryotherapy causes vascular injury and tissue destruction are well known, the molecular mechanisms underlying the fibrinolytic process are not completely understood. Matrix metalloproteinases (MMPs) are a family of zinc-dependent proteases that regulate ECM turnover by processing a wide range of ECM components, such as collagen (20). MMP-2 and MMP-9, in particular, are gelatinases that promote degradation of the ECM. Notably, recent studies on liver fibrosis showed that MMP-9 produced by Kupffer cells, resident hepatic macrophages localized in the lumen of sinusoids, contributes to the resolution of liver fibrosis (11, 21, 22). Specifically, this study used an $MMP9^{-/-}$ animal model to demonstrate that MMP-9 plays a critical role in macrophage-mediated liver fibrillolysis (23). In addition, studies on cardiac wound healing after myocardial infarction also found that deletion of macrophage-derived MMP-9 resulted in increased collagen accumulation (10, 14, 23). Collectively, these studies suggest that macrophage-derived MMPs contribute to ECM destruction in a broad range of fibrotic diseases.

During tissue injury and healing, the changing environment reshapes macrophage phenotypes and provides them with diverse functional properties in each phase of the wound healing process: inflammatory phase, proliferative phase, and maturation phase (24). Distinct macrophage populations that function in tissue remodelling are believed to limit and reverse tissue fibrosis by digesting ECM deposits in the late phase of wound healing. The current study performed histological analysis of keloid tissues and found that $CD163^{+}$ M2 macrophages and MMP-9 are both highly co-expressed in cryotherapy-treated scars. This suggests that superficial cryotherapy may induce the selective recruitment of anti-fibrotic M2 macrophages, which in turn, secrete MMP-9 to facilitate degradation of excessive collagen deposits in keloid scars. Further functional assays should be performed to further investigate the dynamic roles of macrophages in wound healing and fibrotic resolution processes.

In conclusion, these data suggest that M2-like tissue-remodelling macrophages may represent a key factor that orchestrates fibrotic resolution in cryotherapy-treated keloid scars. Although conventional intralesional TA monotherapy is the most convenient method for treating keloid scars, its exclusive use can result in frequent recurrence and high rates of complication. This retrospective study found that combining TA and cryotherapy resulted in greater efficacy, not only for reducing scar volume, but also for improving erythematous colour. We propose that uncovering the mechanism by which cryotherapy induces macrophages to switch to an M2-like phenotype may lead to novel therapeutics for reducing fibrosis in keloid scars.

The authors have no conflicts of interest to declare.

REFERENCES

1. Ogawa R. The most current algorithms for the treatment and prevention of hypertrophic scars and keloids. Plast Reconstr Surg 2010; 125: 557–568.
2. Ogawa R. Keloid and hypertrophic scars are the result of chronic inflammation in the reticular dermis. Int J Mol Sci 2017; 18. pii: E606.
3. Lee YI, Kim J, Yang CE, Hong JW, Lee WJ, Lee JH. Combined therapeutic strategies for keloid treatment. Dermatol Surg 2019; 45: 802–810.
4. Al-Attar A, Mess S, Thomassen JM, Kauffman CL, Davison SP. Keloid pathogenesis and treatment. Plast Reconstr Surg 2006; 117: 286–300.
5. Kafka M, Collins V, Kamolz LP, Rappl T, Branski LK, Wurzer P. Evidence of invasive and noninvasive treatment modalities for hypertrophic scars: a systematic review. Wound Repair

Regen 2017; 25: 139–144.
6. Forbat E, Ali FR, Al-Niaimi F. Treatment of keloid scars using light-, laser- and energy-based devices: a contemporary review of the literature. Lasers Med Sci 2017; 32: 2145–2154.
7. Yosipovitch G, Widijanti Sugeng M, Goon A, Chan YH, Goh CL. A comparison of the combined effect of cryotherapy and corticosteroid injections versus corticosteroids and cryotherapy alone on keloids: a controlled study. J Dermatolog Treat 2001; 12: 87–90.
8. Wong TS, Li JZ, Chen S, Chan JY, Gao W. The efficacy of triamcinolone acetonide in keloid treatment: a systematic review and meta-analysis. Front Med (Lausanne) 2016; 3: 71.
9. Scrimali L, Lomeo G, Tamburino S, Catalani A, Perrotta R. Laser CO2 versus radiotherapy in treatment of keloid scars. J Cosmet Laser Ther 2012; 14: 94–97.
10. Meschiari CA, Jung M, Iyer RP, Yabluchanskiy A, Toba H, Garrett MR, et al. Macrophage overexpression of matrix metalloproteinase-9 in aged mice improves diastolic physiology and cardiac wound healing after myocardial infarction. Am J Physiol Heart Circ Physiol 2018; 314: H224–H235.
11. Feng M, Ding J, Wang M, Zhang J, Zhu X, Guan W. Kupffer-derived matrix metalloproteinase-9 contributes to liver fibrosis resolution. Int J Biol Sci 2018; 14: 1033–1040.
12. Anders CB, Lawton TMW, Ammons MCB. Metabolic immunomodulation of macrophage functional plasticity in nonhealing wounds. Curr Opin Infect Dis 2019; 32: 204–209.
13. Nahrendorf M, Swirski FK. Monocyte and macrophage heterogeneity in the heart. Circ Res 2013; 112: 1624–1633.
14. Yabluchanskiy A, Ma Y, DeLeon-Pennell KY, Altara R, Halade GV, Voorhees AP, et al. Myocardial infarction superimposed on aging: MMP-9 deletion promotes M2 macrophage polarization. J Gerontol A Biol Sci Med Sci 2016; 71: 475–483.
15. Bagabir R, Byers RJ, Chaudhry IH, Muller W, Paus R, Bayat A. Site-specific immunophenotyping of keloid disease demonstrates immune upregulation and the presence of lymphoid aggregates. Br J Dermatol 2012; 167: 1053–1066.
16. Azzam OA, Bassiouny DA, El-Hawary MS, El Maadawi ZM, Sobhi RM, El-Mesidy MS. Treatment of hypertrophic scars and keloids by fractional carbon dioxide laser: a clinical, histological, and immunohistochemical study. Lasers Med Sci 2016; 31: 9–18.
17. Gauglitz GG, Korting HC, Pavicic T, Ruzicka T, Jeschke MG. Hypertrophic scarring and keloids: pathomechanisms and current and emerging treatment strategies. Mol Med 2011; 17: 113–125.
18. Roques C, Teot L. The use of corticosteroids to treat keloids: a review. Int J Low Extrem Wounds 2008; 7: 137–145.
19. Park TH, Cho HJ, Lee JW, Kim CW, Chong Y, Chang CH, et al. Could -79 degrees C spray-type cryotherapy be an effective monotherapy for the treatment of keloid? Int J Mol Sci 2017; 18: 2536.
20. Vandooren J, Van den Steen PE, Opdenakker G. Biochemistry and molecular biology of gelatinase B or matrix metalloproteinase-9 (MMP-9): the next decade. Crit Rev Biochem Mol Biol 2013; 48: 222–272.
21. Ramachandran P, Pellicoro A, Vernon MA, Boulter L, Aucott RL, Ali A, et al. Differential Ly-6C expression identifies the recruited macrophage phenotype, which orchestrates the regression of murine liver fibrosis. Proc Natl Acad Sci U S A 2012; 109: E3186–3195.
22. Gao J, Jiang Z, Wang S, Zhou Y, Shi X, Feng M. Endoplasmic reticulum stress of Kupffer cells involved in the conversion of natural regulatory T cells to Th17 cells in liver ischemia-reperfusion injury. J Gastroenterol Hepatol 2016; 31: 883–889.
23. Chiao YA, Ramirez TA, Zamilpa R, Okoronkwo SM, Dai Q, Zhang J, et al. Matrix metalloproteinase-9 deletion attenuates myocardial fibrosis and diastolic dysfunction in ageing mice. Cardiovasc Res 2012; 96: 444–455.
24. Lech M, Anders HJ. Macrophages and fibrosis: how resident and infiltrating mononuclear phagocytes orchestrate all phases of tissue injury and repair. Biochim Biophys Acta 2013; 1832: 989–997.